

# **MODEL FOR STEEL ENERGY DISSIPATION DEVICES AND EVALUATION OF A DAMAGE-FREE SEISMIC DESIGN STRATEGY**

**Theodore L. Karavasilis**

Assistant Professor of Structural Engineering  
School of Engineering, University of Warwick  
Coventry, United Kingdom

E-mail: [theodore.karavasilis@gmail.com](mailto:theodore.karavasilis@gmail.com)

**Sanaya Kerawala**

Research student  
Department of Engineering Science, University of Oxford  
Oxford, United Kingdom

E-mail: [sanaya.kerawala@exeter.ox.ac.uk](mailto:sanaya.kerawala@exeter.ox.ac.uk)

**George Kamaris**

Research Associate  
Department of Civil Engineering, University of Patras  
Patras, Greece

E-mail: [kamaris@upatras.gr](mailto:kamaris@upatras.gr)

## **1. ABSTRACT**

This paper highlights an alternative seismic design strategy that concentrates damage in removable steel yielding devices and protects the rest of the structural system from yielding. This design strategy is further enhanced by using viscous dampers in parallel to the steel yielding devices. A model for steel yielding devices exhibiting non-degrading hysteretic behaviour, such as slit steel devices, low-strength steel shear panels and buckling restrained braces is proposed. The model is found able to accurately predict the experimentally obtained hysteresis and is implemented in the OpenSees software. A prototype steel building is designed following the proposed seismic design strategy. Seismic analyses show that the building achieves immediate occupancy under the design seismic action and rapid return to occupancy under the maximum considered seismic action.

## **2. INTRODUCTION**

The European seismic code EC8 [1] covers conventional lateral-load resisting systems, such as steel moment-resisting frames (MRFs), designed to experience inelastic deformations in main structural members (beams, columns or braces) under strong earthquakes. These inelastic deformations result in difficult-to-repair damage and

downtime during which the building is repaired and cannot be used or occupied. To overcome these problems, an alternative seismic design strategy that concentrates damage in removable steel yielding devices and protects the rest of the structural system from yielding is highlighted. This design strategy is further enhanced by using viscous dampers in parallel to the steel yielding devices. A model for steel yielding devices exhibiting non-degrading hysteretic behaviour, such as slit steel devices [2], low-strength steel shear panels [3] and buckling restrained braces (BRBs) [4] is proposed. The Bouc-Wen model [5] is modified to simulate combined kinematic and isotropic hardening and is calibrated against existing experimental results. The model is found able to accurately predict the experimentally obtained hysteresis and is implemented in the OpenSees software [6] for use in seismic response analysis of buildings with steel yielding devices. A prototype steel building is designed according to EC8 and EC3 [7] following the proposed seismic design strategy. The results of seismic analyses show that the building achieves immediate occupancy (IO) under the design seismic action (DBE) and rapid return to occupancy (RRO) under the maximum considered seismic action (MCE).

### 3. PROPOSED MODEL FOR STEEL YIELDING DEVICE

The Bouc-Wen model has been used to model steel yielding devices [4]. The model accounts for kinematic hardening (i.e., post-yield force increase with increasing deformation). However, it does not account for the isotropic hardening of steel components under cyclic loading [2-4].

#### 3.1 Mathematical formulation

The force output of the proposed modified Bouc-Wen model is:

$$F = pku + (1 - p)F_y z \quad (1)$$

where  $u$  is the deformation across the element,  $F_y$  the yield force,  $k$  the elastic stiffness,  $p$  is the post-yield stiffness ratio that controls kinematic hardening and  $z$  a dimensionless hysteretic parameter obeying to the nonlinear differential equation

$$\dot{z} = \frac{k}{F_y} \dot{u} \left[ 1 - |z|^n (\beta \operatorname{sgn}(\dot{u}z) + \gamma - \Phi \operatorname{sgn}(\dot{u})(\operatorname{sgn}(z) + \operatorname{sgn}(\dot{u}))) \right] \quad (2)$$

where  $\beta$ ,  $\gamma$  and  $n$  are parameters controlling the shape of the smooth hysteresis,  $\operatorname{sgn}()$  is the signum function, and the overdot denotes derivative with respect to time. The parameter  $\Phi$  controls isotropic hardening and is calculated from

$$\Phi_p = \Phi_{\max,p} \left[ 1 - \exp \left( - p_{\Phi,p} \left| \frac{u_{pl,c}}{u_y} \right| \right) \right] \quad (3.a)$$

or

$$\Phi_n = \Phi_{\max,n} \left[ 1 - \exp \left( - p_{\Phi,n} \left| \frac{u_{pl,c}}{u_y} \right| \right) \right] \quad (3.b)$$

where  $u_{pl,c}$  is the cumulative plastic deformation,  $u_y$  the yield deformation ( $=F_y/k$ ),  $p_{\Phi,p}$  and  $p_{\Phi,n}$  parameters that control the isotropic hardening rate due to cumulative plastic deformation, and,  $\Phi_{\max,p}$  and  $\Phi_{\max,n}$  the maximum possible values of  $\Phi$  for the fully

saturated isotropic hardening condition, i.e., for  $u_{pl.c} \rightarrow \infty$ ,  $\Phi_p \rightarrow \Phi_{\max,p}$  and  $\Phi_n \rightarrow \Phi_{\max,n}$ . On the other hand, when  $u_{pl.c}=0.0$ ,  $\Phi_p=0.0$  and  $\Phi_n=0.0$ .

The current value of the parameter  $\Phi$  is calculated based on the following rules: Eq. (3.a) is used to update  $\Phi_p$  when the deformation increment changes from negative to positive within the plastic region of the hysteresis; Eq. (3.b) is used to update  $\Phi_n$  when the deformation increment changes from positive to negative within the plastic region of the hysteresis;  $\Phi$  equals to  $\Phi_p$  when a positive deformation increment occurs; and  $\Phi$  equals to  $\Phi_n$  when a negative deformation increment occurs.

Typically, yielding devices exhibit the same isotropic hardening in different loading directions [2-3] and hence,  $\Phi_{\max,p} = \Phi_{\max,n}$  and  $p_{\Phi,p} = p_{\Phi,n}$ . However, the model can simulate different isotropic hardening in different loading directions (e.g., BRB hysteresis in [4]) by using different values for the parameters in Eqs. (3.a) and (3.b).

### 3.2 Model calibration against experimental results

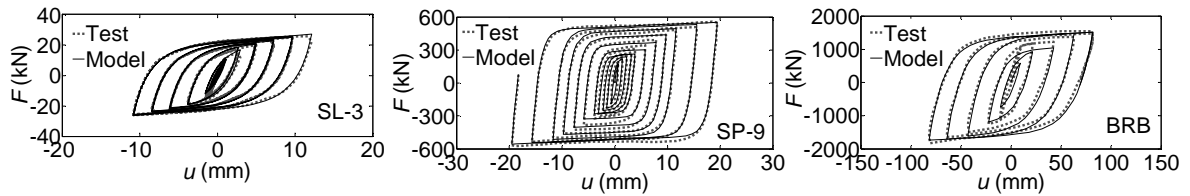


Fig. 1. Test data and results from the proposed model for slit steel devices (left); low-yield steel shear panels (center); and BRBs (right)

Specimen	$F_y$ (kN)	$k$ (kN/mm)	$p$	$\beta$	$\gamma$	$n$	$\Phi_{\max}$	$p_{\Phi}$	$RMS$
Slit device SL-3 in [2]	19.4	9.80	0.040	0.90	0.10	1.0	0.11	0.0130	0.07
Shear panel SP-9 in [3]	224.7	441.9	0.005	0.56	0.44	1.0	0.28	0.0135	0.08
BRB in [4]	1050	93.5	0.0173	0.84	0.16	1.0	0.15 (0.20*)	0.10 (0.15*)	0.13

Table 1. Model parameters calibrated from experimental results ( $\hat{\cdot}$  value of parameter for Eq. (3.b); different isotropic hardening in tension and compression)

The parameters of the model are determined from characterization test data on steel yielding devices available in literature. An unconstrained nonlinear minimization method is used to minimize the root mean square error ( $RMS$ )

$$RMS = \sqrt{\frac{\sum_{i=1}^N (F_i - F_{\exp,i})^2}{\sum_{i=1}^N F_i^2}} \quad (4)$$

where  $N$  is the number of the available experimental force ( $F_{\exp}$ ) data points and  $F$  is the force of the model (see Eq. (1)). Fig. 1 shows test data and results from the proposed hysteretic model for slit steel devices [2], low-yield steel shear panels exhibiting significant isotropic hardening [3] and BRBs exhibiting different isotropic hardening in tension and compression [4]. Table 1 provides information for the test specimens and the

model parameters as well as the RMS values which indicate the accuracy of the proposed model.

### 3.3 Design of slit steel devices

Chan and Albermani [2] designed and tested steel devices fabricated from a short length of an I section with a number of slits cut from the web, leaving a number of strips between the two flanges to deform in flexure and dissipate energy by forming plastic hinges at their ends. As shown in *Fig. 2*, the variables involved in the design of the device are the strip length  $l_0$ , strip depth  $b$  and web thickness  $t$ .

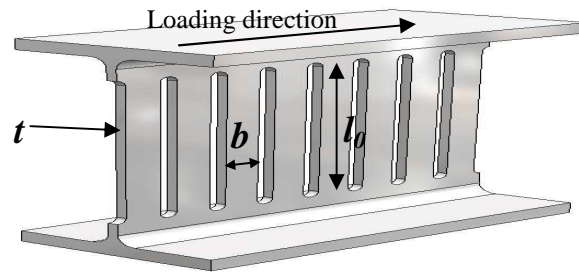


*Fig. 2. Slit steel device designed and tested in [2]*

Based on the analysis presented in [2], the yield strength  $P_y$  of the device is equal to

$$P_y = c_y \frac{n_{st} \sigma_y t b^2}{2l_0} \quad (5)$$

where  $n_{st}$  is the number of strips in the device,  $\sigma_y$  is the yield strength of the material and  $c_y$  is a correction factor to be determined by experimental results. In addition, the elastic stiffness  $k_e$  of the device is calculated through [2]

$$k_e = c_k \frac{n_{st} E t b^3}{l_0^3} \quad (6)$$

where  $E$  is the Young's modulus and  $c_k$  is a stiffness correction factor to be determined by experimental results.

The mean values of the corrections factor  $c_y$  and  $c_k$  were found equal to 1.45 and 0.22, respectively. *Eq. (5)* provides the force level at which the device yields. However, the ultimate strength,  $F_u$ , of the device is needed in order to enable reliable capacity design of the main structural members of the frame (beams, columns and braces). The mean value of the ratio of the ultimate device strength to the yield strength, i.e.,  $F_u/F_y$ , was found equal to 1.32. Another design parameter is the ultimate cyclic deformation capacity  $u_{ult}$  before fracture. Based on the tests presented in [2],  $u_{ult}$  can be approximately considered equal to  $35u_y$ .

## 4. DAMAGE-FREE STEEL BUILDING WITH SLIT DEVICES AND VISCOUS DAMPERS

### 4.1 Prototype building

Fig. 3 (left) shows the plan view of the 5-story, 3-bay by 3-bay prototype office building used for the study. The design study focuses on one perimeter MRF in the N-S direction. This MRF is designed either as a conventional MRF or as an MRF with steel slit devices and viscous dampers in order to compare their seismic response. The slit devices are supported by braces and connected to the bottom flange of the beam. The viscous dampers are inserted in an interior gravity frame (with pin connections) of the building. The MRF with slit devices and the gravity frame with viscous dampers form a hybrid system, referred to herein as the steel MRF with slit devices and viscous dampers, which is shown in Fig. 3 (right). The yield stress of structural steel is equal to 275 MPa. The design response spectrum of the EC8 with a peak ground acceleration of 0.3g and ground type B represents the DBE.

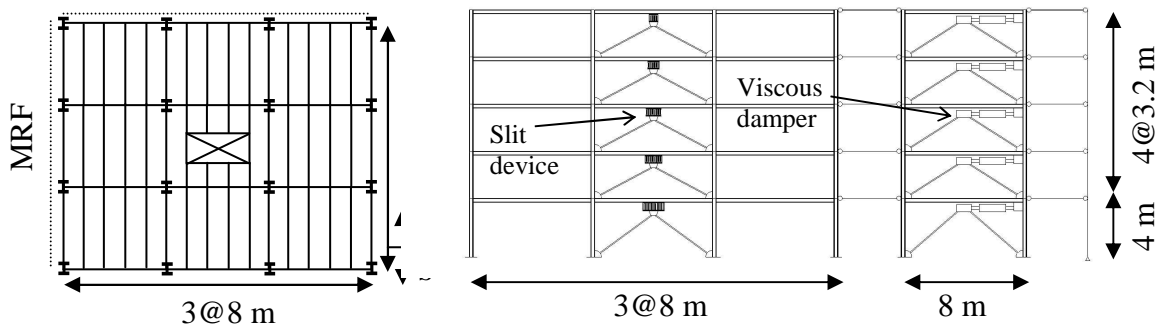


Fig. 3. Prototype building structure: plan view (left); perimeter steel MRF with slit steel devices and interior gravity frame with viscous dampers (right)

#### 4.2 Design of conventional MRF

The perimeter MRF of the building is designed as a conventional steel MRF according to EC3 and EC8. The behaviour factor  $q$  is equal to 6.5. A 0.75% serviceability limit on the peak story drift,  $\theta_{\max}$ , under the frequently occurred earthquake (FOE) with intensity equal to 40% of the intensity of the DBE is adopted.

#### 4.3 Design of steel MRF with slit devices and viscous dampers

The following performance objectives are defined: (1) *IO under the DBE*: The target  $\theta_{\max}$  is set equal to 1% so that: (a) drift-sensitive non-structural elements can avoid damage when designed not to interfere with structural deformations [1]; (b) residual story drifts  $\theta_r$  to be lower than  $0.15 \cdot \theta_{\max} = 0.15 \cdot 1\% = 0.15\%$  [8] and be easily repaired by replacing damaged slit dampers without disturbing building occupation; and (c) main structural members to be damage-free. (2) *RRO under the MCE*: The MCE has intensity 150% the intensity of the DBE and hence,  $\theta_{\max} = 1.5 \cdot 1\% = 1.5\%$  permits to avoid yielding in main structural members, while  $\theta_r = 0.15 \cdot 1.5\% = 0.225\% < 0.5\%$  ensures that repairing slit yielding devices and drift-sensitive non-structural elements will be financially viable [9]. In addition, slit devices should be designed to avoid fracture under the deformations associated with  $\theta_{\max} = 1.5\%$ .

The  $q$  factor is equal to 6.5 and defines the force level at which slit devices are expected to yield. The slit devices dimensions are selected based on Eqs. (5) and (6) in order to provide the required stiffness and strength. Beams, columns and braces are designed to avoid yielding and buckling under the ultimate slit devices forces using standard capacity design rules. Under the DBE, the MRF with slit devices has  $\theta_{\max} = 1.5\%$ . Nonlinear viscous

dampers are designed to provide a supplemental viscous damping ratio  $\xi_s$  equal to 18% according to

$$\xi_s = \frac{\sum_j (2\pi)^a T^{2-a} \lambda_j c_j u_r^{a-1} (\varphi_j - \varphi_{j-1})^{1+a}}{8\pi^3 \sum_j m_i \phi_j^2} \quad (7)$$

where  $j$  denotes a specific story of the MRF,  $a$  is the velocity exponent of the nonlinear viscous dampers (equal to 0.5),  $T$  the fundamental period of vibration,  $\lambda$  a dimensionless parameter,  $c$  the damper constant,  $u_r$  the amplitude of the roof displacement,  $m$  the story mass, and  $\varphi$  the coordinate of the first mode shape [10]. Adding 18% damping to the inherent 2% damping of the MRF provides a response spectrum damping reduction factor equal to 1.5 [10] and hence, the  $\theta_{max}$  under the DBE is reduced to 1.5%/1.5=1.0%.

Story	CONVENTIONAL MRF					MRF WITH SLIT DEVICES AND VISCOUS DAMPERS							
	Column	Beam	$T$ (s.)	Steel weight (kN)	$\theta_{max}$ DBE MCE	Column	Beam	Damper constant $c$ {kN(s./mm) <sup>0.5</sup> }	Slit device geometry: $t/b/l_0$ (mm)	Slit device Number of strips $n_{st}$	$T$ (s.)	Steel weight (kN)*	$\theta_{max}$ DBE MCE
1	HEB400	IPE450	1.70	180	1.75% 2.63%	HEB280	IPE270	33.2	15/66/440	13	1.50	124	1.00% 1.50%
2	HEB400	IPE450				HEB280	PE270	38.0	15/53/350	15			
3	HEB400	IPE400				HEB280	IPE270	34.0	15/53/350	13			
4	HEB360	IPE400				HEB240	IPE240	25.1	15/53/350	10			
5	HEB360	IPE360				HEB240	IPE240	19.1	15/53/350	8			

Table 2. Properties of conventional and proposed steel MRFs (\*Includes the steel weight of the stiff braces used to support slit devices and viscous dampers)

Table 2 provides design details for the conventional MRF and the MRF with slit devices and viscous dampers and shows the significant benefits (lower  $\theta_{max}$  and reduced steel weight) offered by the proposed seismic design strategy. In addition, Table 2 shows that slit devices and nonlinear viscous dampers have cost-effective practical sizes.

## 5. NONLINEAR DYNAMIC ANALYSES

The proposed model for steel yielding devices is implemented in OpenSees and used to model slit devices. Nonlinear viscous dampers are modelled to have a force output  $f_d$

$$f_d = c|v|^a \text{sgn}(v) \quad (8)$$

where  $v$  is the velocity across the damper. A fiber beam column is used to model beams, columns and braces, while nonlinear rotational springs along with kinematic constraints are used to model panel zones. Twenty ground motions scaled to the DBE and MCE level were used for nonlinear dynamic analysis [11]. Fig.4 shows statistics of  $\theta_{max}$  and  $\theta_r$  from nonlinear dynamic analyses and indicates better performance for the MRF with dampers. In addition, the values of  $\theta_{max}$  and  $\theta_r$  are very close to the design target values and confirm that the proposed MRF achieves IO under the DBE and RRO under the MCE.

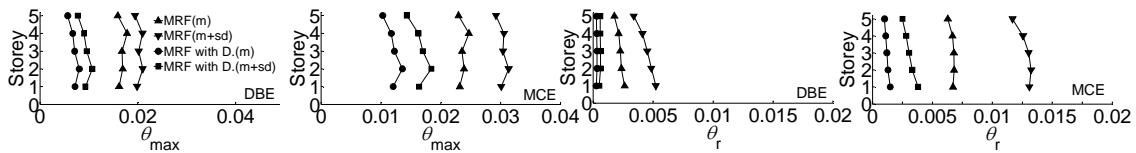


Fig. 4. Statistics of peak story drifts and residual story drifts of the conventional MRF and the MRF with slit devices and viscous dampers

## 5. SUMMARY AND CONCLUSIONS

A seismic design strategy that concentrates damage in removable yielding devices and protects the rest of the structure from yielding with capacity design rules was discussed. This design strategy was further enhanced by using viscous dampers in parallel to the yielding devices. A model for steel yielding devices exhibiting combined kinematic and isotropic hardening was proposed and calibrated against existing experimental results. The results of seismic analyses of a building designed according to the proposed design strategy indicated that the building is able to achieve immediate occupancy under the design seismic action.

## 6. REFERENCES

- [1] CEN. "Eurocode 8: design of structures for earthquake resistance. Part 1: General rules, seismic actions and rules for buildings, 2004.
- [2] Chan, R-WK, Albermani, F, "Experimental study of steel slit damper for passive energy dissipation", *Engineering Structures*, Vol. 30, pp. 1058-1066, 2008.
- [3] Nakashima, M, "Strain-hardening behavior of shear panels made of low-yield steel. I:Test", *Journal of Structural Engineering (ASCE)*, Vol. 121(12), pp. 1742-1749, 1995.
- [4] Merritt, S, Uang, CM, Benzoni, G, "Subassemblage testing of star seismic buckling-restrained braces. Structural Systems Research Project, Report No. TR-2003/04, University of California, San Diego, 2003.
- [5] Wen, YK, "Method for random vibration of hysteretic systems", *Journal of Engineering Mechanics Division*, Vol. 102(2), pp. 249-263, 1976.
- [6] Mazzoni, S, McKenna, F, Scott, M, Fenves, G, "OpenSees. User Command Language Manual", PEER Center, University of California, Berkeley, 2006.
- [7] CEN. "Eurocode 3: design of steel structures. Part 1-1: General rules and rules for buildings", 2005.
- [8] Karavasilis, TL, Seo, CY, "Seismic structural and non-structural performance evaluation of highly damped self-centering and conventional systems", *Engineering Structures*, Vol. 33, p.p. 2248-2258, 2011.
- [9] Mc Cormick, J, Aburano, H, Ikenaga, M, Nakashima, M, "Permissible residual deformation levels for building structures considering both safety and human elements", 14<sup>th</sup> WCEE, Beijing, China, 2008.
- [10] Whittaker, AS, Constantinou, MC, Ramirez, OM, Johnson, MW, Chrysostomou, CZ, "Equivalent lateral force and modal analysis procedures of the 2000 NEHRP Provisions for buildings with damping systems", *Earthquake Spectra*, Vol.19(4), p.p. 959-980, 2003.
- [11] Karavasilis, TL, Kerawala, S, Hale, E, "Hysteretic model for steel energy dissipation devices and evaluation of a minimal-damage seismic design approach for steel buildings", *Journal of Constructional Steel Research*, under review

## **ΜΟΝΤΕΛΟΠΟΙΗΣΗ ΤΗΣ ΥΣΤΕΡΗΤΙΚΗΣ ΣΥΜΠΕΡΙΦΟΡΑΣ ΜΕΤΑΛΛΙΚΩΝ ΑΠΟΣΒΕΣΤΗΡΩΝ ΚΑΙ ΠΡΟΤΑΣΗ ΜΕΘΟΔΟΛΟΓΙΑΣ ΑΝΤΙΣΕΙΣΜΙΚΟΥ ΣΧΕΔΙΑΣΜΟΥ ΜΗΔΕΝΙΚΗΣ ΒΛΑΒΗΣ**

Η παρούσα εργασία επικεντρώνεται σε μία εναλλακτική στρατηγική αντισεισμικού σχεδιασμού η οποία βασίζεται στη χρήση μεταλλικών αποσβεστήρων και κανόνων ικανοτικού σχεδιασμού για τη πλήρη αποφυγή βλάβης στα κύρια δομικά στοιχεία της κατασκευής. Η συγκεκριμένη μεθοδολογία αντισεισμικού σχεδιασμού ενισχύεται περαιτέρω μέσω της χρήσης προστιθέμενης ιξώδους απόσβεσης. Η εργασία αρχικά προτείνει ένα νέο μοντέλο προσομοίωσης της υστερητικής συμπεριφοράς μεταλλικών αποσβεστήρων. Το μοντέλο προσομοιώνει με ακρίβεια πειραματικά αποτελέσματα ανακυκλιζόμενης φορτισης μεταλλικών αποσβεστήρων και υλοποιείται προγραμματιστικά ως νόμος μη γραμμικής συμπεριφοράς στο λογισμικό OpenSees. Ένα μεταλλικό κτίριο σχεδιάζεται με βάση την προτεινόμενη στρατηγική αντισεισμικού σχεδιασμού. Μη γραμμικές δυναμικές αναλύσεις αποδεικνύουν ότι το κτίριο επιτυγχάνει επιτελεστικότητα άμεσης επαναφοράς σε κανονική χρήση υπό τη σεισμική δράση σχεδιασμού.